Electronic Supplementary Material (ESI) for Nanoscale.

Controllable synthesis of $MoS_2@MoO_2$ nanonetwork to boost NO_2 room temperature sensing in air

Muhammad Ikram,[a†] Lujia Liu,[a†] Yang Liu,[a] Mohib ullah,[a] Laifeng Ma,[a] Syed ul Hasnain Bakhtiar,[a] Hongyuan Wu,[b] Haitao Yu,[a] Ruihong Wang,*[a] and Keying Shi *[a]

Abstract: the supporting information provided shows: (i) TEM and HRTEM images of the as prepared MSO-1 nanocomposite, (ii) TEM and HRTEM images of MSO-3 nanocomposite, (iii), (iv), (v) TEM and HRTEM images of the flower like MoS_2 NSs, thin MoO_2 and thin MoO_3 nanoplates respectively, (vi) SEM images of the flower like MoS_2 NSs and of the MoO_3 thin nanoplates, (vii) EDS spectra and mapping of the MSO-2, (viii) XRD pattern of the MoO_3 nanoplates, (ix) XPS analysis of the pure MoS_2 NSs, (x) Fitted impedance parameters of the samples (xi) stability of the MSO-2 and of the pure MoS_2 NSs in air, (xii) response-recovery curve of the as fabricated samples, (xiii) calibration curve of MSO-2, and response/recovery time all of the sensors, (xiv) humidity effect, (xv) table of the comparative response and response/recovery time all of the samples, (xvi) Band diagram of the MoS_2 and MoO_2 before contact, (xvii) comparison of the present study with reported work.

Table of contents

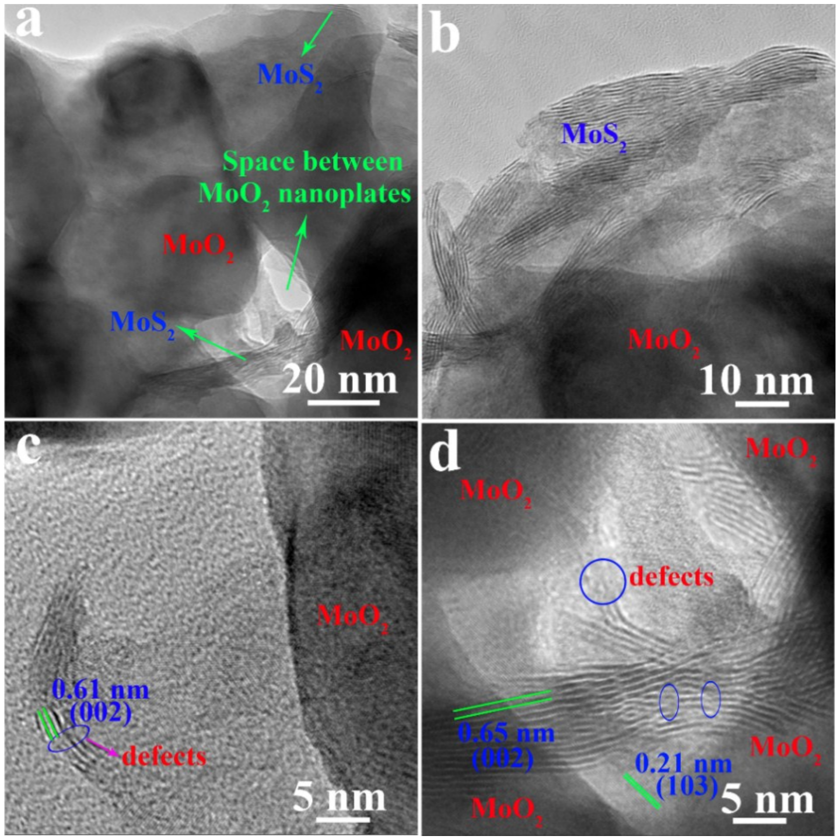

Fig. S1 (a) TEM image; (b-d) HRTEM images of MSO-1 nanocomposite (green line: MoS_2). HRTEM images showing defects and heterostructure interfaces).

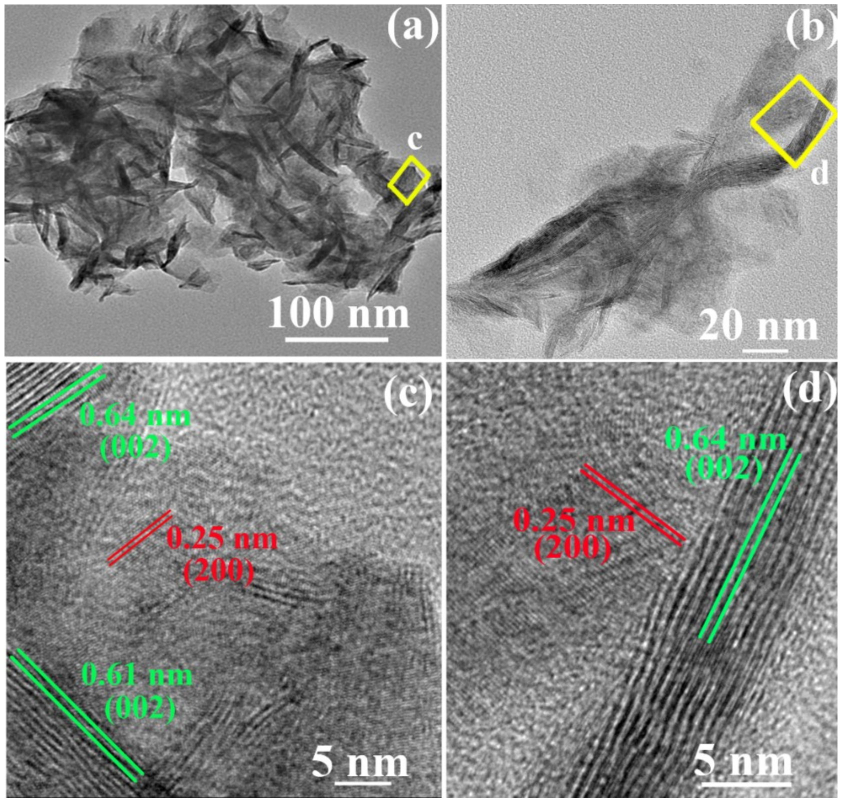

Fig. S2 (a, b) TEM images (c, d) HRTEM images of MSO-3 nanocomposite (green line: MoS_2; red line: MoO_2).

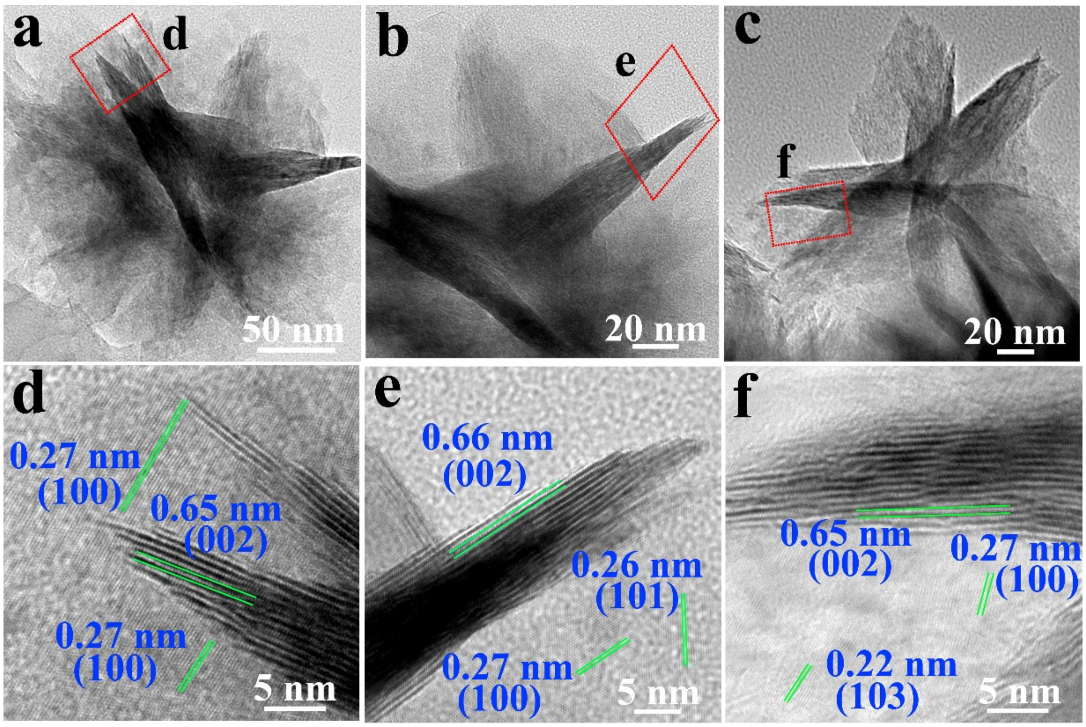

Fig. S3 (a-c) TEM images of flower like pure MoS_2 NSs; (d-f) HRTEM images of (a), (b) and (c).

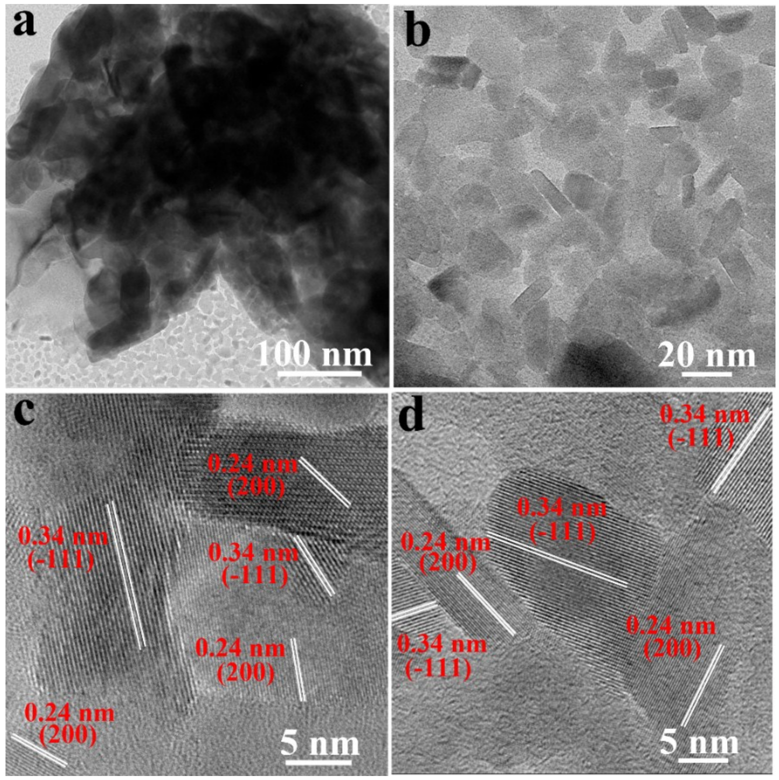

Fig. S4 (a, b) TEM images of pristine MoO_2 thin nanoplates; (c, d) HRTEM images of (a) and (b).

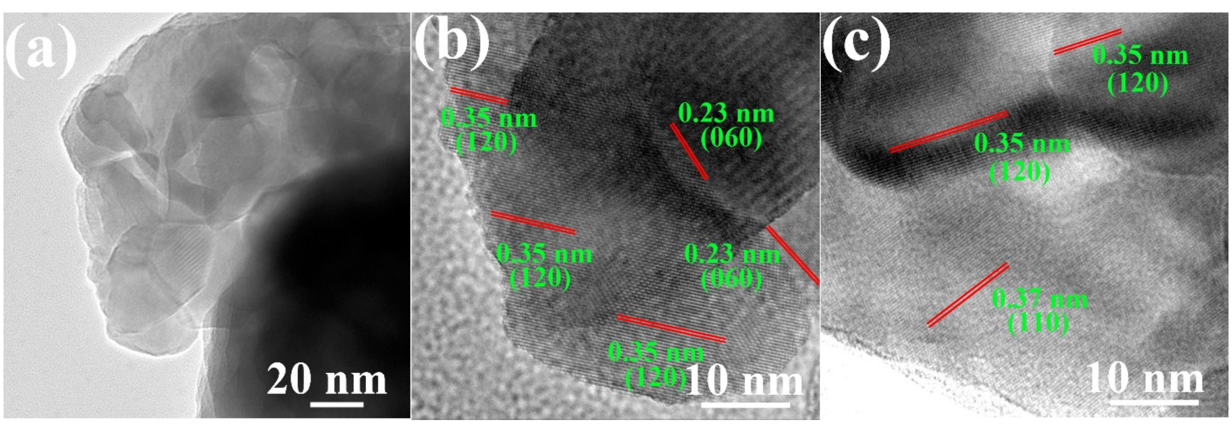

Fig. S5 (a) TEM images of MoO_3 thin nanoplates; (c, d) HRTEM images.

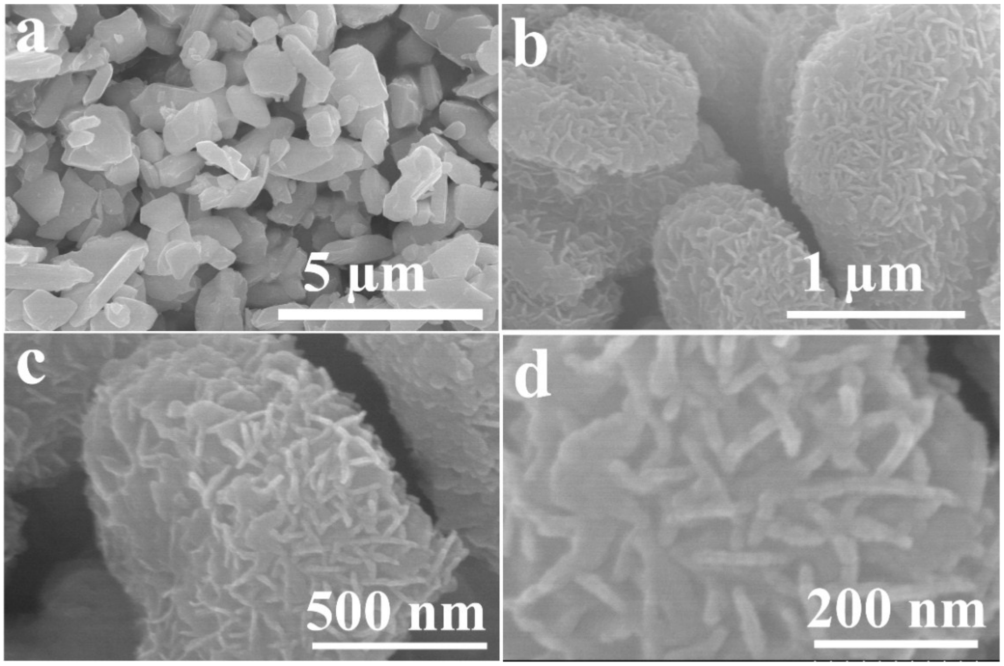

Fig. S6 SEM images of (a) Pure MoO_3; (b-d) MoS_2 NSs (which were formed with sulfurization of MoO_3 for 2 h).

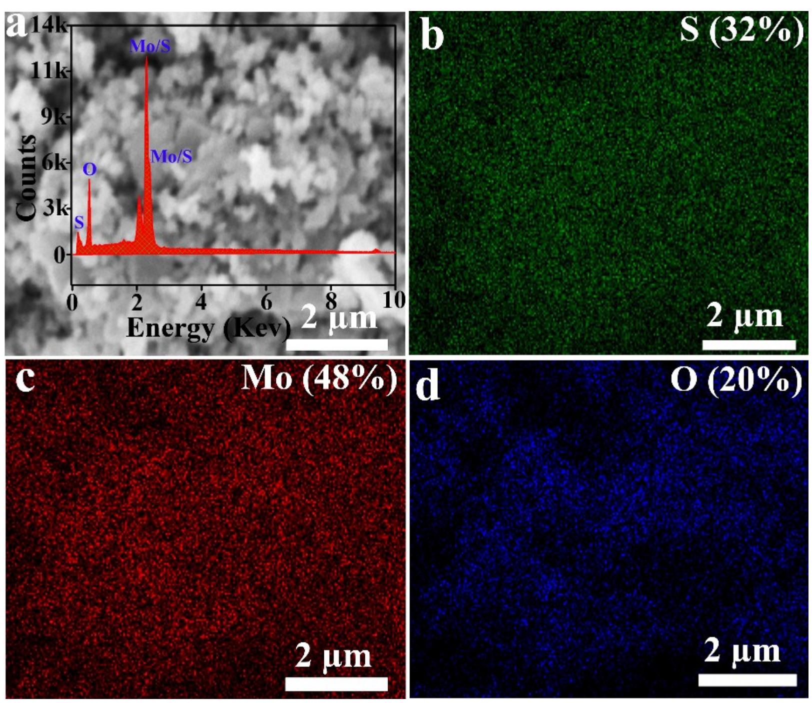

Fig. S7 (a) SEM image, EDS spectra (inset in (a)) and elemental mapping of MSO-2.

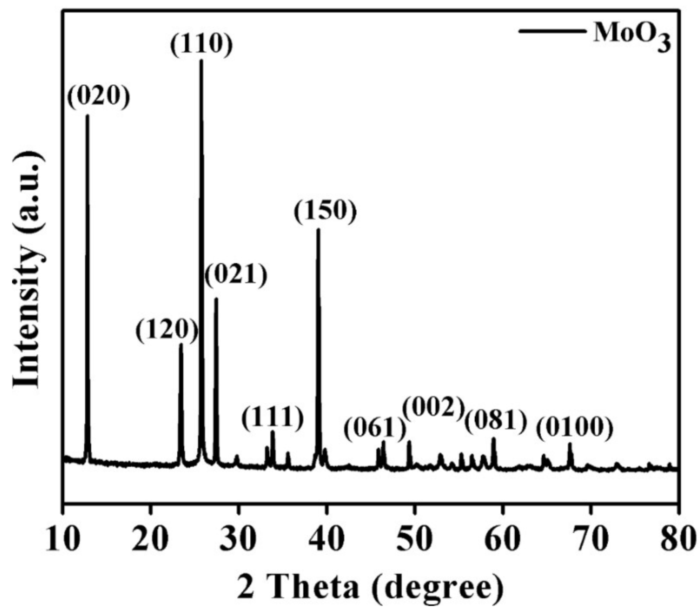

Fig. S8 XRD diffraction pattern of MoO_3.

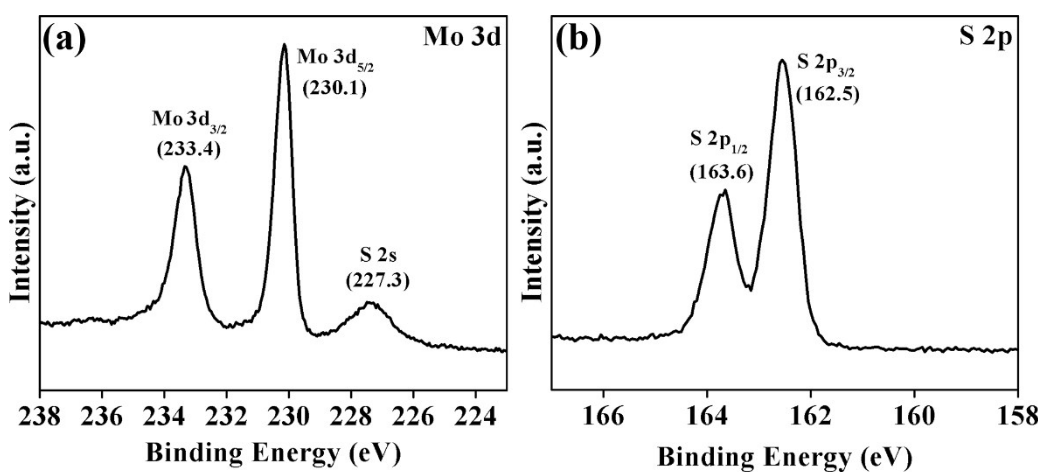

Fig. S9 (a, b) XPS spectra of Mo 3d and S 2p, respectively of the pure MoS_2 NSs.

Table S1. Fitted impedance parameters of samples

Samples	MoS_2	MoO_2	MSO-2
R_{Ω} (Ω)	74.4	69.1	45.3
R_{ct} (Ω)	7336	5145	1041

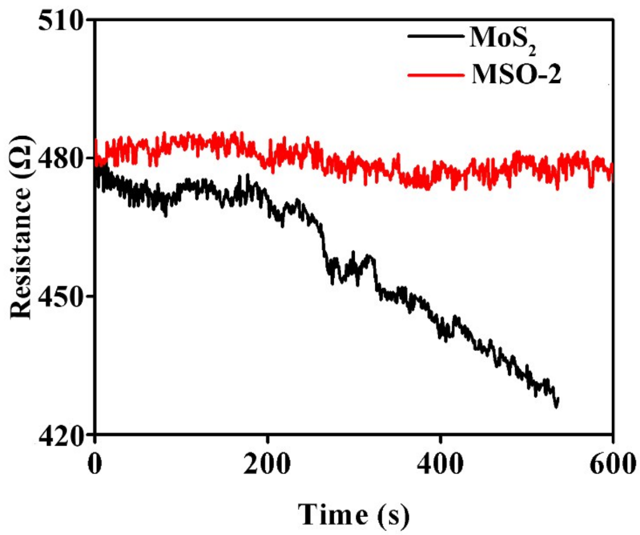

Fig. S10 The resistance of the MSO-2 sensor compared with pure MoS_2 sensor in air at RT, indicating the high stability of MSO-2 nanonetworks sensor compare to pure MoS_2 sensor.

As shown in Fig. S10, the pure MoS_2 is highly unstable in air and also in NO_2 atmosphere at RT, and the resistance of the devices increasingly shifting to lower compared to MSO-2 nanonetworks.

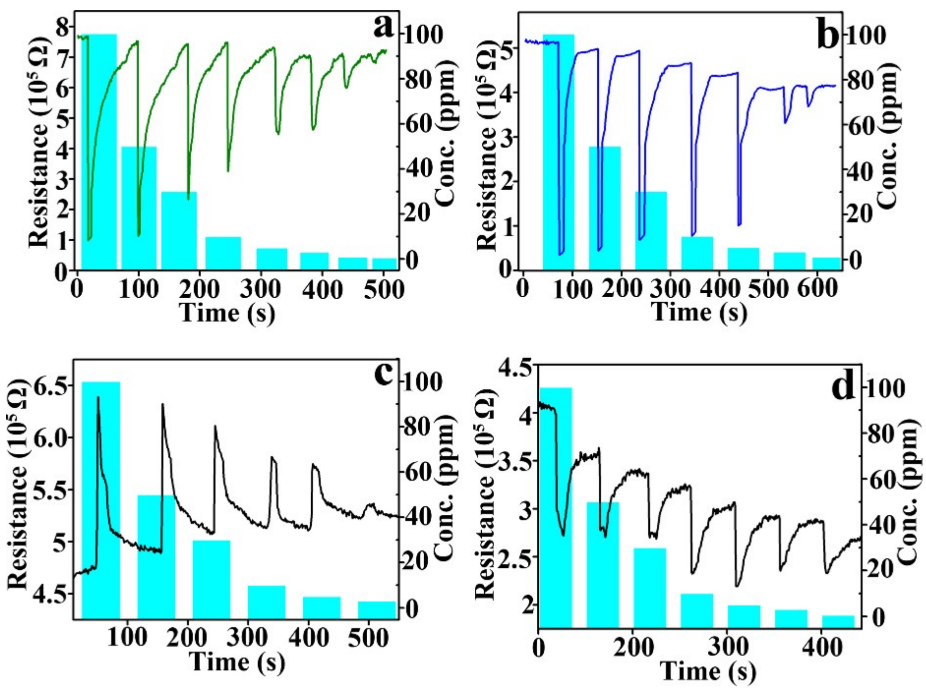

Fig. S11 The response-recovery curve of (a) MSO-1, (b) MSO-3, (c) pure MoO_2, (d) pure MoS_2 to NO_2 gas at RT in air.

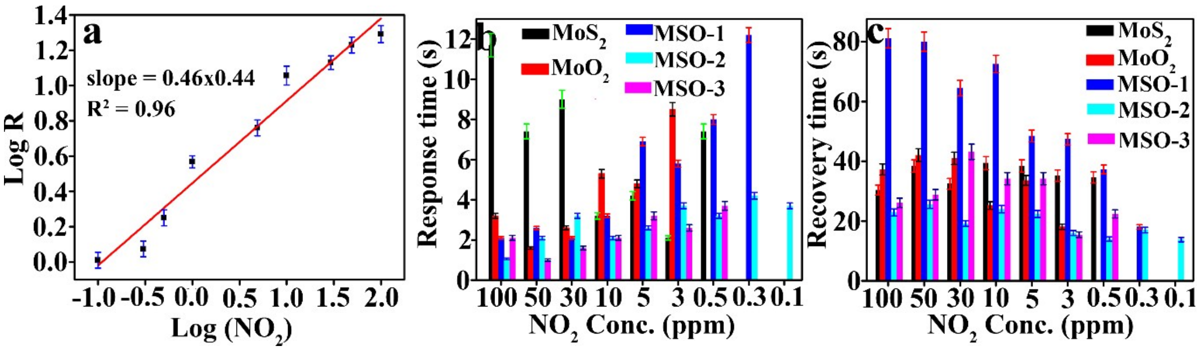

Fig. S12 (a) The calibration curve of MSO-2 sensor to 0.1-100 ppm NO_2; (b, c) Response time and recovery time all of the sensors.

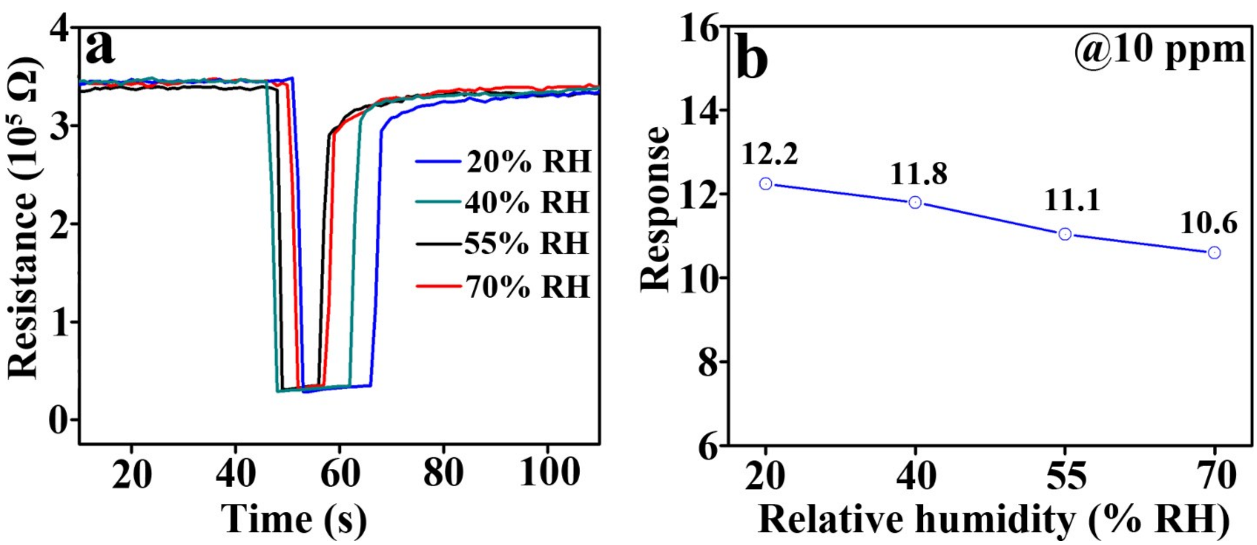

Fig. S13 (a) The transient response-recovery of MSO-2 sensor to 10 ppm NO_2 in different humidity; (b) Response to 10 ppm NO_2 as a function of the relative humidity.

Table S2. Response, response time and recovery time of the sensors to NO_2 at room temperature.

Sensors	MoS_2			MoO_2			MSO-1			MSO-2			MSO-3		
NO_2 (ppm)	Response	T_s	T_r	Response	T_s	T_r	Response	T_s	T_r	Response	T_s	T_r	Response	T_s	T_r
100	1.47	11.7	30.4	1.32	3.2	37.3	7.79	2.1	81.1	**19.43**	**1.06**	**22.9**	14.73	2.1	26.1
50	1.34	7.4	38.4	1.28	1.6	42.1	6.44	2.6	80.0	**17.30**	**2.1**	**25.6**	11.22	1.0	28.8
30	1.25	9.0	32.5	1.19	2.6	41.0	3.18	2.1	64.5	**13.71**	**3.2**	**19.2**	7.29	1.6	43.2
10	1.39	3.2	39.4	1.12	5.3	25.2	2.29	3.2	72.5	**12.33**	**2.1**	**24.0**	6.01	2.1	34.2
5	1.40	4.2	38.4	1.11	4.8	33.6	1.63	6.9	48.5	**5.81**	**2.6**	**22.4**	4.41	3.2	34.2
3	1.24	2.1	35.2	1.02	8.5	18.1	1.52	5.8	47.4	**3.84**	**3.7**	**16.0**	1.12	2.6	15.4
0.5	1.22	7.4	34.6				1.18	8.0	37.3	**1.79**	**3.2**	**14.0**	1.09	3.7	22.4
0.3							1.04	12.2	18.1	**1.12**	**4.2**	**17.0**			
0.1										**1.03**	**3.7**	**13.8**			

T_s = Response Time (s), T_r = Recovery Time (s)

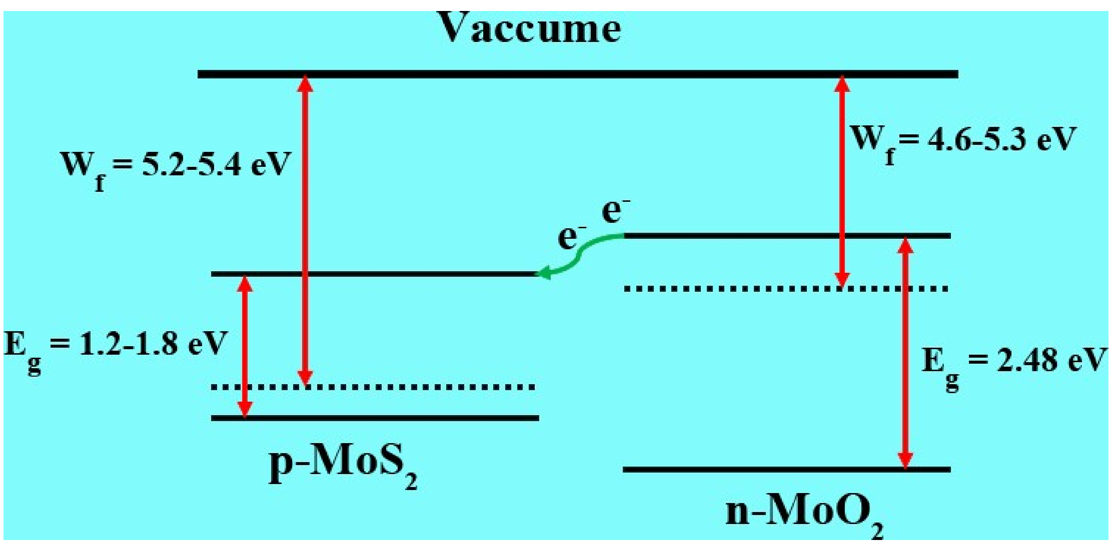

Scheme S1. Band diagram of MoS_2 and MoO_2 before contact.

Table S3. Comparison of the Gas-Sensing Performances of the $MoS_2@MoO_2$ Nanonetwork toward NO_2 with Previous Works.

Sensing material	NO_2 conc. (ppm)	Operation temperature (°C)	Response/Recovery time (s)	Ref.
MoS_2 microspheres	100	150	79/225	1
MoS_2 flakes	100	RT(UV)	29/350	2
3D MoS_2 aerogel	1	200	33/107	3
2D MoS_2	500	RT	180/480	4
MoS_2/ZnO hetero-nanostructure	5	RT	40/40	5
MoS_2–MoO_3	10	RT	19/182	6
MoS_2/Graphene Hybrid Aerogel	1	200	21.6/29.4	7
MoS_2/SnO_2	10	RT	408/162	8
RGO-MoS_2-CdS nanocomposite	0.2	75	25/34	9
ZnO/rGO nanocomposite	1	RT	75/132	10
Graphene-SnO_2 nanocomposite	5	150	129/107	11
2D SnS_2	10	120	170/140	12
SnS_2/SnO_2 nanoheterojunctions	1	100	299/143	13
$MoS_2@MoO_2$ nanonetwork	100/0.1	RT	1.06/22.9 (100 ppm) 3.7/13.8 (0.1 ppm)	This work

References

(1) Y. Li, Z. Song, Y. Li, S. Chen, S. Li, Y. Li, H. Wang and Z. Wang, *Sens. Actuators B: Chem*. 2019, **282**, 259-267.

(2) R. Kumar, N. Goel, and M. Kumar, *ACS Sens*. 2017, **2**, 1744-1752.

(3) H. Long, L. Chan, A. H. Trochimczyk, L. E. Luna, Z. Tang, T. Shi, A. Zettl, C. Carraro, M. A. Worsley, and R. Maboudian, *Adv. Mater. Interfaces*, 2017, **4**, 1700217.

(4) Y. Zhao, J. G. Song, G. H. Ryu, K. Y. Ko, W. J. Woo, Y. Kim, D. Kim, J. H. Lim, S. Lee, Z. Lee, J. Park and H. Kim, *Nanoscale*, 2018, **10**, 9338–9345.

(5) Y. Han, D. Huang, Y. Ma, G. He, J. Hu, J. Zhang, N. Hu, Y. Su, Z. Zhou, Y. Zhang, and Z. Yang, *ACS Appl. Mater. Interfaces*, 2018, **10**, 22640−22649.

(6) R. Kumar, N. Goel, M. Mishra, G. Gupta, M. Fanetti, M. Valant, and M. Kumar, *Adv. Mater. Interfaces*, 2018, **5**, 1800071.

(7) H. Long, A. H. Trochimczyk, T. Pham, Z. Tang, T. Shi, A. Zettl, C. Carraro, M. A. Worsley, and R. Maboudian, *Adv. Funct. Mater*. 2016, **26**, 5158-5165.

(8) S. Cui, Z. Wen, X. Huang, J. Chang and J. Chen, *Small*, 2015, **11**, 2305-2313.

(9) S. Shao, L. Che, Y. Chen, M. Lai, S. Huang and R. Koehn, *J. Alloys and Comp*., 2019, 774, 1-10.

(10) Y. Xia, J. Wang, J. Xu, X. Li, D. Xie, L. Xiang and S. Komarneni, *ACS Appl. Mater. Interfaces*, 2016, **8**, 35454−35463.

(11) H. W. Kim, H. G. Na, Y. J. Kwon, S. Y. Kang, M. S. Choi, J. H. Bang, P. Wu and S. S. Kim, *ACS Appl. Mater. Interfaces,* 2017, **9**, 31667-31682.

(12) J. Z. Ou, W. Ge, B. Carey, T. Daeneke, A. Rotbart, W. Shan, Y. Wang, Z. Fu, A. F. Chrimes, W. Wlodarski, S. P. Russo, Y. X. Li and K. K. zadeh, *ACS Nano*, 2015, **9**, 10313-10323.

(13) J. Hao, D. Zhang, Q. Sun, S. Zheng, J. Sun and Y. Wang, *Nanoscale*, 2018,**10**, 7210-7217.